Carrier heating in light-emitting quantum-dot heterostructures at low injection currents

Janik Wolters,[1] Matthias-René Dachner,[1,*] Ermin Malić,[1] Marten Richter,[1] Ulrike Woggon,[2] and Andreas Knorr[1]
[1]*Institut für Theoretische Physik, Nichtlineare Optik und Quantenelektronik, Technische Universität Berlin, Hardenbergstraße 36, EW 7-1 10623 Berlin, Germany*
[2]*Institut für Optik und Atomare Physik, Technische Universität Berlin, Strasse des 17. Juni 135 ER 1-1, 10623 Berlin, Germany*
(Received 2 October 2009; published 2 December 2009)

We present microscopic calculations of the light emission and carrier dynamics in an electrically pumped quantum-dot emitter at low injection currents and room temperature. The modeled structure consists of a bulk semiconductor and self organized InGaAs/GaAs quantum-dot layers (embedded by a wetting layer). Carrier transport through the structure is driven by scattering with longitudinal optical phonons including the nonequilibrium phonon dynamics. Even though the phonon distribution remains at room temperature, a substantial carrier heating corresponding to more than 50 K above the phonon temperature occurs in the wetting layer. Surprisingly, this temperature difference is observed in particular at low pump currents. It can be attributed to a nonequilibrium in the sample due to energy level alignment and external pumping.

DOI: 10.1103/PhysRevB.80.245401 PACS number(s): 78.67.Hc, 42.55.Sa, 72.10.Di, 73.23.−b

I. INTRODUCTION

Quantum-dot emitters (QDEs) consist of QDs embedded into the intrinsic layer of *p*-*i*-*n* diode structures. These devices have two main applications. (i) High speed optical networks require electrically pumped semiconductor amplifiers[1,2] and lasers.[3] Recent efforts focus on the construction of ultrafast devices with low power consumption. The latter task mainly aims at reducing the lasing threshold current and is of particular importance in highly integrated photonic networks. (ii) At low, modulated pumping currents quantum key distribution for methods in quantum cryptography is a proposed QDE application.[4] Here, most of the current approaches rely on single and entangled photons,[5–7] i.e., nonclassical light, and ultimately rely on photon sources at low pumping currents. For both application fields, i.e., lasers and nonclassical light sources, QDEs with self assembled QDs are the most elaborated candidates.[8,9] A detailed theoretical understanding of the microscopic electron transfer and photon emission processes in a QDE is essential for future optimization and development.

QDEs consist of a spatial extended, three-dimensional bulk of intrinsic or doped semiconductor with several layers of QDs (cf. Fig. 1). Due to the self-assembling growth mechanism,[8,10] the investigated QDs are not directly embedded in the surrounding bulk material, but are located in a thin, i.e., two-dimensional wetting layer (WL). Light is emitted by radiative electron-hole recombinations from confined QD levels (Fig. 1). In order to induce such recombination processes, carriers must be injected into the bulk semiconductor first. This is usually done via *p*-*n* contacts sandwiching the bulk-WL-QD system. From the bulk material carriers relax via the WL into the QDs to recombine there radiatively.

Phonon-assisted WL-QD transition has been assumed to be a bottleneck in the relaxation chain,[11,12] since phonon-assisted transitions between discreet QD states are energetically forbidden. Here, we will use a multiphonon approach to describe this transition.[13,14]

In the following, we examine the main idea of this paper by analyzing the consequences of the energy alignment, cf. Fig. 1(b), in the considered QD structures. Potential energy of bulk electrons/holes is transformed into kinetic energy of WL carriers when carriers are scattered from the bulk band structure minima into the WL. After injection, these high energetic WL carriers will lose energy by emission of phonons. A detailed analysis of the WL-QD scattering shows that mainly carriers around the WL Γ point, i.e., carriers with low kinetic energy are scattered into the QD. Therefore, during its operation via electrical pumping, the WL is permanently filled with carriers of high energy, while carriers with low energy are drained to the QDs. Compared to an equilibrium situation, the WL carrier distribution is deformed in favor of the high energy tail. Later on, we will show that this distribution—even if it is a nonequilibrium distribution—can be fitted by a Fermi–Dirac distribution and it is justified to define a temperature in terms of the mean free energy. The deformation of the carrier distribution corresponds to a heating of the WL carriers. Since the scattering probability from the WL to the QD depends strongly on the WL temperature,[2,14] this heating will influence the device performance.

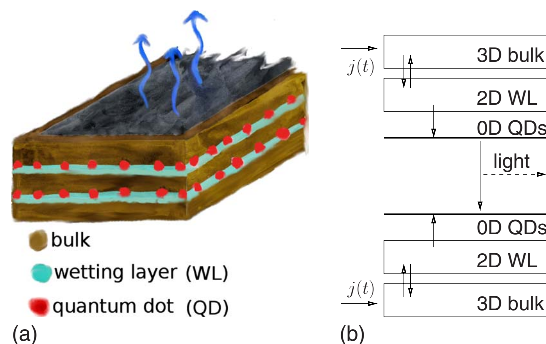

FIG. 1. (Color online) (a) Schematic view of a QD photo emitter with two active layers. (b) Energy level scheme of the investigated structure. The energetic difference between the lowest states in bulk and WL is 64 meV (187 meV) for electrons (holes). The QD electron (hole) states are in a distance of 79 meV (42 meV) from the WL band edge. The lens-shaped QDs have typically a diameter of 10 nm and a height of 5 nm (Ref. 8).

 ©2009 The American Physical Society

TABLE I. Physical parameters of bulk GaAs.

Constant	Symbol	Value
Low-frequency dielectric number	ε_l	12.9
High-frequency dielectric number	ε_h	10.9
Effective electron mass	$m_{\text{bulk,e}}$	$0.067m_0$
Effective hole mass	$m_{\text{bulk,h}}$	$0.51m_0$
LO phonon energy	$\hbar\omega_{\text{LO}}$	36.4 meV

To study the proposed heating effects, we investigate a model structure to evaluate the coupled electron-phonon dynamics to analyze a carrier heating in QDE, in particular at low electrical pump currents.

II. MODEL QDE STRUCTURE

The considered QDE [Fig. 1(a)] consists of a GaAs bulk semiconductor and Stranski-Krastanov grown InAs QDs embedded in a two-dimensional $In_{0.5}Ga_{0.5}As$ WL forming a quantum well.[8,15] A list of used material parameters can be found in Tables I and II. Later, we discuss how the results can be applied to QDEs with several active layers. Maintaining a low externally injected current, the transport through the structure is driven by microscopic scattering of nonequilibrium carriers with longitudinal-optical (LO) phonons (Fröhlich coupling).[2,16]

We focus on weakly pumped devices operating with low carrier densities at room temperature. Here, carrier-LO phonon scattering clearly dominates the dynamics. Coulomb scattering, important at high carrier densities, i.e., above 10^{10} cm^{-2} in the WL,[16] is neglected in our study due to a low carrier density assumption. This leads to carrier level occupations $\ll 1$. By incorporation of Coulomb interaction, our approach can be expanded to the high injection regime.

Referring to Fig. 1(b), carriers are electrically injected into the bulk semiconductor, from where they relax via the WL states into the QDs. The pumping into the bulk material is realized by carrier reservoirs.[17] The expansion of the bulk material in growth direction is assumed to be 500 nm and thus large enough to neglect quantum confinement effects. In the bulk material the carrier wave functions $|\Psi_{\text{bulk}}\rangle$ are plane Bloch waves and the corresponding energies (i.e., parabolic dispersion). Around the Γ point of the band structure can be obtained using the effective mass approximation. In contrary, the states inside the wetting layer are quantum confined in growth direction, while unconfined in perpendicular dimensions. Using the envelope function approximation[18] the confinement potential is approximated by an one-dimensional infinite square well with an effective width L_{eff}.[19] In the investigated setup, at the Γ point only a single subband with the wave function $|\Psi_{\text{WL}}\rangle$ has an energy below the bulk band edge.

TABLE II. Physical parameters of the $In_{0.5}Ga_{0.5}As$ WLs.

Constant	Symbol	Value
Effective electron mass	$m_{\text{WL,e}}$	$0.042251m_0$
Effective hole mass	$m_{\text{WL,h}}$	$0.461m_0$
Effective WL width	L_{eff}	8 nm

The lens shaped QDs have typically a diameter of 10 nm and a height of 5 nm.[8] Thus the wave functions $|\Psi_{\text{QD}}\rangle$ are quantum confined in all three spatial dimensions. The confinement in growth direction is modeled via an infinite square well, while the in-plane wave function is approximated by a two-dimensional harmonic oscillator. This is a good approximation for dots with a small aspect ratio.[20]

Interactions between the states are determined by wave function overlap. Since bulk, WL, and QD states are not independent from each other, but eigenfunctions of the same single particle Hamiltonian, they have to be orthogonal. In particular, in the case of bulk-well and well-dot coupling the matrix elements are overestimated by the use of plane wave functions.[21] To calculate the combined bulk-well and well-dot scattering matrix elements, orthogonal plane waves $|\tilde{\Psi}_\alpha\rangle$ are used[21]

$$|\tilde{\Psi}_\alpha\rangle = N^{-1/2}\left[|\Psi_\alpha\rangle - \sum_{\alpha'\neq\alpha}|\Psi_{\alpha'}\rangle\langle\Psi_{\alpha'}|\Psi_\alpha\rangle\right].$$

Here, the sum runs over all nonorthogonalized states $|\Psi_\alpha\rangle$, while the normalization factor N is chosen in a way that $\langle\tilde{\Psi}_\alpha|\tilde{\Psi}_\alpha\rangle = 1$.

The LO phonons are assumed to have GaAs bulklike properties with a constant energy $\hbar\omega_{\text{LO}}$, independent of their wave vector $\vec{q}$ according to the Einstein model.

III. HAMILTONIAN

The Hamilton operator consists of three parts, $\mathcal{H} = \mathcal{H}_{\text{free}} + \mathcal{H}_{\text{c-phonon}} + \mathcal{H}_{\text{c-photon}}$, where the first part describes the free-carrier contribution as well as the free phonon and photon fields

$$\mathcal{H}_{\text{free}} = \sum_\alpha \varepsilon_\alpha a_\alpha^\dagger a_\alpha + \hbar\omega_{\text{LO}}\sum_\beta b_\beta^\dagger b_\beta + \hbar\omega c^\dagger c. \quad (1)$$

Here, $a_\alpha^\dagger$ (a_α) is the fermionic carrier creation (annihilation) operator. The compound index α contains the carrier type (electron or hole), the subsystem (bulk: $\alpha \in$ bulk, ith WL: $\alpha \in$ WL, or jth QD in the ith WL: $\alpha \in$ QD), and, if necessary, the carrier momentum $\vec{k}$. The latter is a three-dimensional vector in the case of bulk carriers, while it is two dimensional within the WL. α also contains the spin, which we implicitly include in the $\vec{k}$ sums since all considered interactions are spin diagonal and spin-orbit coupling turns out to be weak for the energy scales involved in this investigation.[22]

$b_\beta^\dagger$ (b_β) is the bosonic creation (annihilation) operator of LO phonons with a three-dimensional wave vector $\vec{q_\beta}$. For the interaction between carriers and light, only a single mode in a leaky cavity, described by the photon creation (annihilation) operator $c^\dagger$ (c) is taken into account.

The second contribution of $\mathcal{H}$ is the carrier-phonon Hamilton operator

$$\mathcal{H}_{\text{c-phonon}} = \sum_{\alpha\alpha'\beta} (g^{\beta}_{\alpha,\alpha'} a^{\dagger}_{\alpha} a_{\alpha'} b_{\beta} + \text{H.c.}). \quad (2)$$

The Fröhlich carrier-phonon coupling elements $g^{\beta}_{\alpha,\alpha'}$ are given by[18]

$$g^{\beta}_{\alpha,\alpha'} = -i\sqrt{\frac{2\pi e^2\hbar\omega}{\gamma V}}\frac{1}{|q_{\beta}|}\langle\Psi_{\alpha}|e^{i\vec{q}_{\beta}\vec{r}}|\Psi_{\alpha'}\rangle. \quad (3)$$

The coupling strength is defined by the chosen wave functions and the material parameters, cf. Tables I and II. Here, γ is the effective dielectric constant of GaAs bulk material: $\gamma=\varepsilon_0(\frac{1}{\varepsilon_h}-\frac{1}{\varepsilon_l})^{-1}$. If the states $|\Psi_{\alpha}\rangle$ and $|\Psi_{\alpha'}\rangle$ both are three-dimensional plane waves, the expectation value in Eq. (3) provides momentum conservation, otherwise it yields the form factor $\mathcal{F}=\langle\Psi_{\alpha}|e^{iq_{\beta}r}|\Psi_{\alpha'}\rangle$ for bulk-WL and WL-QD interaction.

The carrier-light interaction Hamiltonian reads in the electron-hole picture[23]

$$\mathcal{H}_{\text{c-photon}} = \sum_{\alpha,\alpha'} (M_{\alpha,\alpha'} a_{\alpha} a_{\alpha'} c^{\dagger} + \text{H.c.}). \quad (4)$$

The carrier light interaction described by $\mathcal{H}_{\text{c-photon}}$ is restricted to the QD states. The coupling matrix element $M_{\alpha,\alpha'}$ is nonvanishing, only if α and α' refer to different carrier types, i.e., electrons and holes, in the same QD.

IV. EQUATIONS OF MOTION FOR CARRIER TRANSPORT AND PHOTON EMISSION

To describe the electron-phonon scattering processes, which drive the electrons through the compound system, a higher order Born approach to the many particle correlations in the bulk, WL, and QD systems is applied.[14,24,25] The equations of motion for an arbitrary operator O are derived through the Heisenberg equation: $i\hbar\partial_t O=[O,H]_-$. Expectation values of observables are calculated using the density matrix ρ

$$\langle O\rangle = \text{tr}(\rho O). \quad (5)$$

We start with the carrier dynamics and discuss the photon emission dynamics later on.

A. Electron transport

Applying a standard equations of motion approach[26] the Markovian dynamics of the carrier populations $f_{\alpha}=\text{tr}(\rho a^{\dagger}_{\alpha} a_{\alpha})$, and phonon occupation numbers $n_{\beta}=\text{tr}(\rho b^{\dagger}_{\beta} b_{\beta})$ (ρ being the initial statistical operator) are given by Boltzmann-type rate equations[18,27]

$$\frac{\partial}{\partial t} f_{\alpha} = \Gamma^{\text{in}}_{\alpha}(1-f_{\alpha}) - \Gamma^{\text{out}}_{\alpha} f_{\alpha}, \quad (6)$$

$$\frac{\partial}{\partial t} n_{\beta} = \Gamma^{+}_{\beta}(1+n_{\beta}) - \Gamma^{-}_{\beta} n_{\beta}. \quad (7)$$

The corresponding relaxation processes are illustrated in Fig. 2. The considered channels are relaxation within the bulk and the WL states, carrier scattering from bulk to WL states, and phonon-assisted capture into the QDs. The in and out scattering rates $\Gamma^{\text{in/out}}_{\alpha}$ and the emission (+) and absorption (−) rates $\Gamma^{\pm}_{\beta}$ are functions of the carrier and phonon distribution functions and are calculated microscopically. We use second order Born-Markov approximation for the bulk-WL coupling. This approach results in the Bloch-Boltzmann-Peierls formulas, Eqs. (6) and (7) (Refs. 18, 27, and 28) with the scattering rates

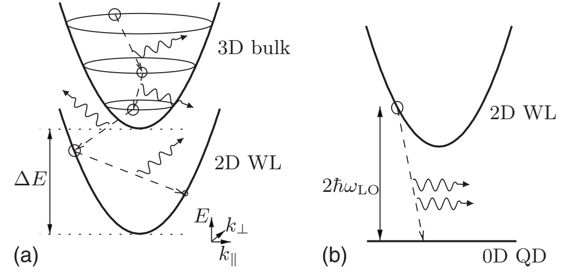

FIG. 2. Scattering channel of the investigated system. (a) Possible relaxation process of an excited bulk electron into the WL. By emission of one phonon, the electron loses always the energy $\hbar\omega_{\text{LO}}$. In all processes that include a WL state the perpendicular momentum $k_{\perp}$ is not conserved. (b) Relaxation from the WL into the QD. A carrier can only scatter from a resonant WL state, i.e., a state with integer times the phonon energy from the QD state, emitting several phonons.

$$\Gamma^{\text{in}}_{\alpha} = \frac{2\pi}{\hbar^2}\sum_{\substack{\alpha',\beta\\ \pm}} |g^{\beta}_{\alpha,\alpha'}|^2 f_{\alpha'}\left(n_{\beta}+\frac{1}{2}\pm\frac{1}{2}\right)\delta(\Delta^{\pm}_{\alpha,\alpha'}), \quad (8)$$

$$\Gamma^{\text{out}}_{\alpha} = \frac{2\pi}{\hbar^2}\sum_{\substack{\alpha',\beta\\ \pm}} |g^{\beta}_{\alpha,\alpha'}|^2 (1-f_{\alpha'})\left(n_{\beta}+\frac{1}{2}\pm\frac{1}{2}\right)\delta(\Delta^{\mp}_{\alpha,\alpha'}) \quad (9)$$

for scattering within and between WL and bulk. The energy differences $\Delta^{\pm}_{\alpha,\alpha'}$ are defined by $\hbar\Delta^{\pm}_{\alpha,\alpha'}=\epsilon_{\alpha}-\epsilon_{\alpha'}\pm\hbar\omega_{\beta}$ and the term $|g^{\beta}_{\alpha,\alpha'}|^2$ results from second order Born approximation. The factor $(n_{\beta}+\frac{1}{2}\pm\frac{1}{2})$ accounts for absorption (−) or spontaneous and stimulated emission (+) of phonons. Similarly, the emission rates Γ^{+}_{β} and absorption rates Γ^{-}_{β} for LO phonons in the mode β are given by

$$\Gamma^{\pm}_{\beta} = \frac{2\pi}{\hbar^2}\sum_{\alpha,\alpha'} |g^{\beta}_{\alpha,\alpha'}|^2 f_{\alpha}(1-f_{\alpha'})\delta(\Delta^{\pm}_{\alpha,\alpha'}). \quad (10)$$

In principle, the sums in Eqs. (8) and (9) run over all electronic states of the system, but most of the terms vanish due to momentum conservation included in the matrix elements or energy conservation, preserved by the Dirac-Delta function. Allowed processes are depicted in Fig. 2.

For the QD-WL interaction a second order Born approximation breaks down.[29] In particular, scattering into the QD states are energetically forbidden due to the large energy offset of the lowest WL states to the bound QD states. Such transitions cannot be described by single phonon processes. However, the WL-QD scattering is of great importance for

the device dynamics, since it feeds the optical active QD transitions. To address this problem, we use projection-operator-based effective many phonon Hamiltonians[14,30,31] for carrier capture processes into the quantum dots. This corresponds to a higher order virtual state description within a higher order Born approximation. Again, one obtains a Boltzmann-type equation of motion

$$\frac{\partial}{\partial t} f_{\alpha\in \mathrm{QD}} = \Gamma^{\mathrm{in}}_{\alpha}(1 - f_{\alpha\in \mathrm{QD}}) - \Gamma^{\mathrm{out}}_{\alpha} f_{\alpha\in \mathrm{QD}} \tag{11}$$

Here, we omit the resulting out scattering rate $\Gamma^{\mathrm{out}}_{\alpha\in \mathrm{QD}}$ for dot states, since its contribution is negligible.[14] The in scattering is driven by occupied wetting layer states $f_{\alpha'}$ with the energy $\epsilon_{\alpha'}$ close to the resonant energy $\epsilon^{\mathrm{res}}_{\alpha} = \epsilon_{\alpha\in \mathrm{QD}} + n\hbar\omega$, which is resonant to the n-phonon process

$$\Gamma^{\mathrm{in}}_{\alpha\in \mathrm{QD}} = \frac{1}{\tau_\alpha} \sum_{\alpha'\in \mathrm{WL}} f_{\alpha'} \mathcal{L}(\epsilon_{\alpha'} - \epsilon^{\mathrm{res}}_{\alpha}) \tag{12}$$

Quasiparticle broadening via acoustic phonons, lifetime broadening, and inhomogeneous broadening is included by the distribution function $\mathcal{L}(\epsilon_{\alpha'} - \epsilon_{\mathrm{res}})$. For numerical reasons we approximate the coupling of all WL states with $\epsilon_{\alpha'} \le \hbar\omega_{\mathrm{LO}}$ equally to the QDs. This is valid since inhomogeneous broadening is in the same range as a LO phonon energy.[32] The scattering into QDs corresponds to an out scattering from the WL states. The corresponding WL equation of motion reads

$$\left.\frac{\partial}{\partial t} f_{\alpha'\in \mathrm{WL}}\right|_{\mathrm{QD}} = -\underbrace{\frac{1}{\tau_\alpha}(1 - f_{\alpha\in \mathrm{QD}})}_{\Gamma^{\mathrm{out,QD}}_{\alpha'}} f_{\alpha'}, \quad \epsilon_{\alpha'} \le \hbar\omega_{\mathrm{LO}}. \tag{13}$$

For the total out scattering rate $\Gamma^{\mathrm{out,QD}}_{\alpha'}$ we calculated $\Gamma^{\mathrm{out,QD}}_{\alpha'} = 3\ \mathrm{ps}^{-1}$ for holes and $\Gamma^{\mathrm{out,QD}}_{\alpha'} = 0.3\ \mathrm{ps}^{-1}$ for electrons.

To describe realistic, electrically pumped structures, electrical carrier injection from the p-n contacts is included by coupling the bulk to pump reservoir distributions $f^{\mathrm{pump}}_{\alpha}(t)$, where the Fermi levels in the reservoirs are variable by external bias of the device.[17] This approach results in additional injection rates for the bulk states

$$\Gamma^{\mathrm{in,pump}}_{\alpha\in \mathrm{bulk}} = \eta^{\alpha} f^{\mathrm{pump}}_{\alpha}(t), \tag{14}$$

$$\Gamma^{\mathrm{out,pump}}_{\alpha\in \mathrm{bulk}} = \eta^{\alpha}[1 - f^{\mathrm{pump}}_{\alpha}(t)]. \tag{15}$$

The $f^{\mathrm{pump}}_{\alpha}$ correspond to reservoir states with the same momentum as the corresponding $f_{\alpha\in \mathrm{bulk}}$. The injection efficiency $\eta^{\alpha} = 10^{-7}\ \mathrm{s}^{-1}$ is constant for all electron states, while the efficiency η^{α} for the hole states is adjusted dynamically between 0 and 10^{-8}, to obtain global charge neutrality.

Carrier generation and carrier losses in the bulk and the WLs are included in form of phenomenological rates. The loss rate in the bulk is $\Gamma^{\mathrm{out,gr}}_{\alpha\in \mathrm{bulk}} = 1\ \mathrm{ns}^{-1}$ and for the WL $\Gamma^{\mathrm{out,gr}}_{\alpha\in \mathrm{WL}} = 10\ \mathrm{ns}^{-1}$.[18]

Additionally we take into account repulsion of the phonon occupation into the equilibrium by anharmonic decay. In accordance with experiments this time constant is $\tau^{\mathrm{decay}}_{\mathrm{phonon}} = 3.5\ \mathrm{ps}$.[33]

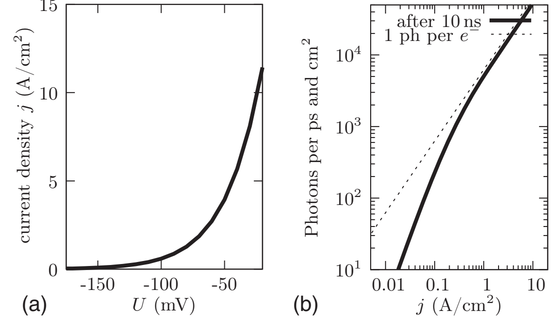

FIG. 3. (a) The current-voltage characteristics is typical for a diodelike structure. (b) Losses play only a minor role and the photon emission is close to the one photon per electron-hole pair limit. At extreme low currents it takes longer than 10 ns to reach a steady state.

B. Summary of the equations of motion

Altogether, we obtain the final set of equations

$$\frac{\partial}{\partial t} f_\alpha = \tilde{\Gamma}^{\mathrm{in}}_{\alpha}(1 - f_\alpha) - \tilde{\Gamma}^{\mathrm{out}}_{\alpha} f_\alpha, \tag{16}$$

$$\frac{\partial}{\partial t} n_\beta = \Gamma^{+}_{\beta}(1 + n_\beta) - \Gamma^{-}_{\beta} n_\beta - \frac{n_\beta - n_{\beta,0}}{\tau^{\mathrm{decay}}_{\mathrm{phonon}}}, \tag{17}$$

where the total scattering rates $\tilde{\Gamma}^{\mathrm{in/out}}_{\alpha}$ are the sums of the individual rates

$$\tilde{\Gamma}^{\mathrm{in/out}}_{\alpha} = \Gamma^{\mathrm{in/out}}_{\alpha} + \Gamma^{\mathrm{in/out,pump}}_{\alpha} + \Gamma^{\mathrm{in/out,gr}}_{\alpha} \tag{18}$$

and $n_{\beta,0}$ is the equilibrium phonon distribution. The coupled differential equations Eqs. (16) and (17) can be solved numerically using standard methods.

C. Photon emission

Knowing the dynamics of the populations directly leads to the photon output of a QD-based device. Taking into account a radiative recombination constant τ_{rad}, leads to an estimation of the photon flux. In the limiting case of low photon density and the weak coupling limit, the carrier-light Hamiltonian, Eq. (4), yields the spontaneous emission of photons from occupied quantum-dot states[34]

$$\frac{d}{dt} n^{\mathrm{pt}} = 2N_{\mathrm{QD}} \frac{f_{\mathrm{QD,e}} f_{\mathrm{QD,h}}}{\tau_{\mathrm{rad}}} - \frac{n^{\mathrm{pt}}}{\tau_{\mathrm{loss}}}. \tag{19}$$

The photon occupation is damped by a cavity loss $\tau_{\mathrm{loss}} = 4\ \mathrm{ps}$.[35] The photon creation is proportional to the number of QDs N_{QD}, and the factor of two results from spin degeneracy.

V. NUMERICAL RESULTS

By applying a constant voltage, the Fermi levels in the pump reservoirs are adjusted and after several nanoseconds a stationary current flows through the structure [Fig. 3(a)]. The current density j is calculated by summing up the pump

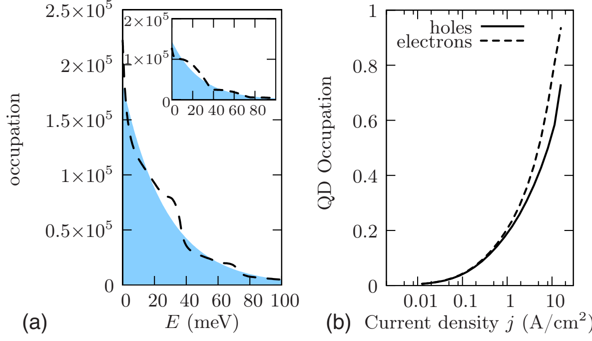

FIG. 4. (Color online) (a) Electron distribution in the quantum well. The filled curve shows the assigned Fermi function. Inset: hole distribution with same axes. (b) The QD occupation increases with increasing current.

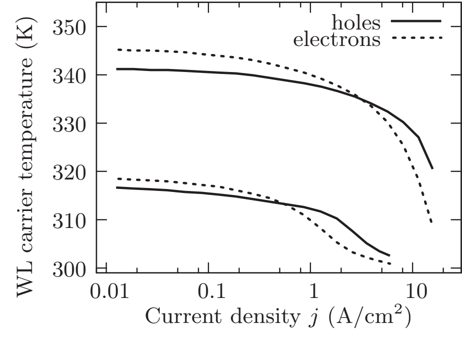

FIG. 5. The carrier temperature in the structure decreases with increasing current. The dot density of the structure from the upper curves is 5×10^{10} and 1×10^{10} cm^2 for the lower curves.

terms over all bulk electron state and multiplying with the elementary charge e (Ref. 17)

$$j=\frac{e}{A_{\mathrm{WL}}}\sum_{\alpha\in\mathrm{bulk}}[\Gamma_{\alpha}^{\mathrm{in,pump}}(1-f_{\alpha})-\Gamma_{\alpha}^{\mathrm{out,pump}}f_{\alpha}]. \qquad (20)$$

Figure 3(b) shows the photon emission in continuous operation. At extreme low currents, in the few photon regime it takes longer than 10 ns to reach the steady state. Thus the calculated emission stays below the theoretical limit of one photon per electron-hole pair.

We now focus on the microscopic information contained in our model: under steady, nonequilibrium operation, the carriers in the bulk and the WLs deviate from an ideal Fermi distribution at room temperature [Fig. 4(a)]. However, their distribution is close to a Fermi-Dirac function at higher temperature and thus it is justified to define a temperature for comparison with a quasi-Fermi function at room temperature. A temperature of the WL carriers can be defined easily by the expectation values of the total carrier energy $\langle E_{tot}\rangle=\Sigma_{\vec{k}}\frac{\hbar^2\vec{k}^2}{2m_{\mathrm{eff}}}f_{\vec{k}}$ and the particle number $\langle N_{tot}\rangle=\Sigma_{\vec{k}}f_{\vec{k}}$. Using these values a temperature T can be attributed to the carrier distributions. In terms of that for bulk carriers the classical Boltzmann limit is even valid. In this case, the bulk carrier temperature T can be calculated by using

$$\langle E_{tot}\rangle=\frac{3}{2}\langle N_{tot}\rangle\beta^{-1}. \qquad (21)$$

Here, the inverse temperature β is defined by $\beta=(k_BT)^{-1}$ with k_B being the Boltzmann constant.

In the two-dimensional wetting layer this classical limit appears to be invalid. However, we find the exact expression

$$\langle E_{tot}\rangle=-\frac{C}{\beta^2}\mathrm{Li}_2\left[1-\exp\left(\frac{\langle N_{tot}\rangle\beta}{C}\right)\right] \qquad (22)$$

for the free energy of a two-degree electron gas. The constant C is defined by $C=\frac{m_{\mathrm{eff}}A_{\mathrm{WL}}}{\pi\hbar^2}$ and $\mathrm{Li}_2[z]$ is the dilogarithm of z with: $\mathrm{Li}_2[z]=\Sigma_{k=1}^{\infty}\frac{z^k}{k^2}$. From Eq. (22) the temperature can be obtained numerically.

In the following we focus on the device relevant room temperature. In steady operation, the temperatures of the bulk carriers and the LO phonons remain at their initial value of 300 K. At least in the studied low injection limit, the generation of nonequilibrium LO phonons is too weak to influence the dynamics. Note, that other two-dimensional systems, with a stronger electron-phonon coupling, e.g., graphene, exhibit phonon heating due to carrier relaxation.[28]

Since the impact of WL dynamics to the bulk phonons is negligible, the approach can be linearly extrapolated to several WL-QD layers. In the WL a substantial heating of the two-dimensional electron gas occurs. Figure 5 depicts the evaluated WL carrier temperature as a function of injection current. We observe a QD density dependent carrier heating, in particular for low injection currents This heating originates from the permanent nonequilibrium pumping from the bulk into the WL: in the injection process carriers gain kinetic energy due to the potential difference between bulk and wetting layer states. Therefore, typically carriers with high kinetic energies are injected into the WL, while the QDs act as a sink for carriers with low kinetic energy, around the Γ point of the band structure. The average energy is elevated in the WL carrier distribution, i.e., the temperature is increased. As a surprising effect, we find, that the heating is more pronounced at low currents and vanishes at higher currents, cf. Fig. 5. This clearly means, that it depends on the time, an electron spends in the WL whether heating occurs or not. If carriers are instantly transferred to the dots after reaching the Γ point, there are only few electrons with low energy in the WL, i.e., the WL distribution is hot, or vice versa if carriers remain in the WL before being transferred. To check this interpretation, we define the average carrier dwell time $\tau_{\mathrm{WL}}^{\lambda}$ in the wetting layer by the ratio of the current density j and the density of carriers $n_{\mathrm{WL}}^{\lambda}=\frac{1}{A_{\mathrm{WL}}}\Sigma_{\alpha\in\mathrm{WL}}f_{\alpha,\lambda}$ of type $\lambda=\{\mathrm{electron},\ \mathrm{hole}\}$ in the WL

$$\tau_{\mathrm{WL}}^{\lambda}=\frac{n_{\mathrm{WL}}^{\lambda}}{j}. \qquad (23)$$

The defined dwell time is the time needed to transfer the number of carriers stored in the WL, $A_{\mathrm{WL}}n_{\mathrm{WL}}^{\lambda}$, by the current $A_{\mathrm{WL}}j$ through the WL.

Calculations for various QD densities and currents show, that the carrier temperature in the WL is a function of the dwell time $\tau_{\mathrm{WL}}^{\lambda}$, cf. Fig. 6. At low dwell times the carriers do

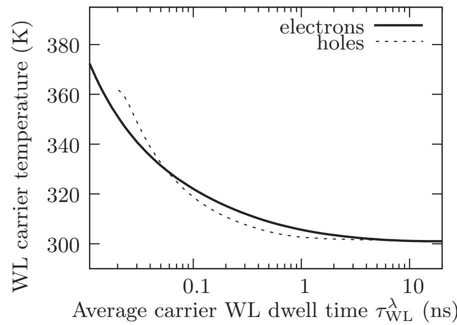

FIG. 6. The carrier temperature in quantum wells is a function of the carrier dwell time $\tau^{\lambda}_{\mathrm{WL}}$, defined in Eq. (23).

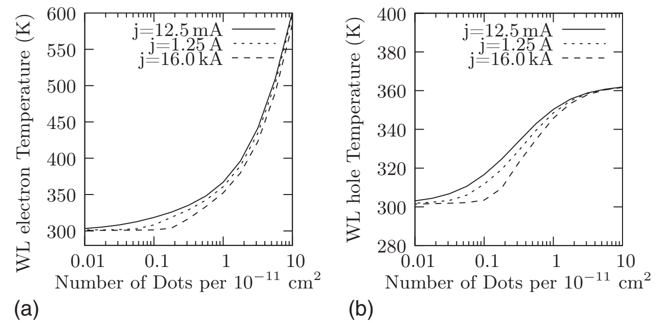

FIG. 7. (a) The electron temperature in the quantum well in dependence of the quantum-dot density at different currents. The current is normalized on a QDE with an active area of 1 cm^2 and one active layer, operating at $T_0=300$ K. (b) Temperature of holes in the quantum well.

not have the time to cool within the WL. Now, we can understand the current-temperature characteristics from Fig. 5. Since the dwell time is determined by the ratio of $n^{\lambda}_{\mathrm{WL}}$ and j, one may expect the dwell time to decrease and thus the temperature to raise with increasing current. But due to Pauli blocking in the QD states [Fig. 4(b)] the WL density increases faster than linear with the current. Therefore, increasing current leads to an increased dwell time and to a reduced heating since the carriers acquire time to cool via phonon emission. We note, that the proposed heating mechanism is in agreement with earlier experiments on the cooling time in quantum wells from Ref. 36.

The WL carrier temperature, or alternatively $\tau^{\lambda}_{\mathrm{WL}}$, is also very sensitive to the dot density (Fig. 7). This is caused by the direct influence of the dot density on the out scattering rate. Above 1×10^{10} QDs per cm^2, a value easily achieved in experiments,[15] the temperature raises at small currents as shown in Fig. 7. Even values around 600 K can be reached for electrons. The hole temperature does not reach as high values. The temperature saturates since a maximum temperature is defined by the pumping distribution. The hole temperature saturates for smaller number of dots than the electron temperature, since the drain per dot is much higher for holes than for electrons.

VI. CONCLUSION

We have calculated the coupled carrier-phonon dynamics for a biased light emitter device built up from a heterostructure of bulk, wetting layer, and quantum dots. We investigated the limit of low injection currents and single photon emission, using microscopically based equations of motion. The electrons and holes in the bulk and the wetting layer appear to have different temperatures. In particular at low dwell times the carriers in the wetting layers do not have time to cool and a substantial carrier heating well above room temperature is predicted. The impact of this heating influences on the device performance, such as for emitters of nonclassical light working in this limit,[37] will be discussed in further research.

ACKNOWLEDGMENTS

We acknowledge for financial support by Deutsche Forschungsgemeinschaft (DFG) through Sonderforschungsbereich (SFB) 787 “Nanophotonik.”

*dachner@itp.physik.tu-berlin.de

[1] S. Dommers, V. V. Temnov, U. Woggon, J. Gomis, J. Martinez-Pastor, M. Lämmlin, and D. Bimberg, Appl. Phys. Lett. **90**, 033508 (2007).
[2] J. Gomis-Bresco, S. Dommers, V. V. Temnov, U. Woggon, M. Lämmlin, D. Bimberg, E. Malić, M. Richter, E. Schöll, and A. Knorr, Phys. Rev. Lett. **101**, 256803 (2008).
[3] F. Hopfer, A. Mutig, M. Kuntz, G. Fiol, D. Bimberg, N. N. Ledentsov, V. A. Shchukin, S. S. Mikhrin, D. L. Livshits, I. L. Krestnikov, A. R. Kovsh, N. D. Zakharov, and P. Werner, Appl. Phys. Lett. **89**, 141106 (2006).
[4] O. Benson, C. Santori, M. Pelton, and Y. Yamamoto, Phys. Rev. Lett. **84**, 2513 (2000).
[5] N. Akopian, N. H. Lindner, E. Poem, Y. Berlatzky, J. Avron, D. Gershoni, B. D. Gerardot, and P. M. Petroff, Phys. Rev. Lett. **96**, 130501 (2006).
[6] K. Hennessy, A. Badolato, M. Winger, D. Gerace, M. Atature, S. Gulde, S. Falt, E. L. Hu, and A. Imamoglu, Nature (London) **445**, 896 (2007).
[7] P. Michler, Top. Appl. Phys. **90**, 315 (2003).
[8] D. Bimberg, M. Grundmann, and N. N. Ledentsov, *Quantum Dot Heterostructures* (John Wiley & Sons, New York, 1999).
[9] S. Scheel, J. Mod. Opt. **56**, 141 (2009).
[10] D. Leonard, M. Krishnamurthy, C. M. Reaves, S. P. Denbaars, and P. M. Petroff, Appl. Phys. Lett. **63**, 3203 (1993).
[11] J. Urayama, T. B. Norris, J. Singh, and P. Bhattacharya, Phys. Rev. Lett. **86**, 4930 (2001).
[12] R. Heitz, H. Born, F. Guffarth, O. Stier, A. Schliwa, A. Hoffmann, and D. Bimberg, Phys. Rev. B **64**, 241305(R) (2001).
[13] T. Inoshita and H. Sakaki, Phys. Rev. B **46**, 7260 (1992).
[14] M.-R. Dachner, E. Malić, M. Richter, A. Carmele, J. Kabuß, A. Wilms, J.-E. Kim, G. Hartmann, J. Wolters, U. Bandelow, and A. Knorr (unpublished).
[15] V. M. Ustinov, N. A. Maleev, A. R. Kovsh, and A. E. Zhukov, Phys. Status Solidi A **202**, 396 (2005).
[16] M. Lorke, T. R. Nielsen, J. Seebeck, P. Gartner, and F. Jahnke,

Phys. Rev. B **73**, 085324 (2006).

[17] W. W. Chow and S. W. Koch, IEEE J. Quantum Electron. **41**, 495 (2005); W. W. Chow, A. Knorr, S. Hughes, A. Girndt, and S. W. Koch, IEEE J. Sel. Top. Quantum Electron. **3**, 136 (1997).

[18] H. Haug and S. W. Koch, *Quantum Theory of the Optical and Electronic Properties of Semiconductors*, 3rd ed. (World Scientific, Singapore, 2001); E. Schöll, *Nonlinear Spatio-Temporal Dynamics and Chaos in Semiconductors*, Nonlinear Science Series, Vol. 10 (Cambridge University Press, Cambridge, England, 2001).

[19] A. Liu, Phys. Rev. B **50**, 8569 (1994).

[20] A. Wójs, P. Hawrylak, S. Fafard, and L. Jacak, Phys. Rev. B **54**, 5604 (1996).

[21] H. C. Schneider, W. W. Chow, and S. W. Koch, Phys. Rev. B **64**, 115315 (2001); **70**, 235308 (2004);

[22] M. Vachon, S. Raymond, A. Babinski, J. Lapointe, Z. Wasilewski, and M. Potemski, Phys. Rev. B **79**, 165427 (2009).

[23] M. Richter, S. Butscher, M. Schaarschmidt, and A. Knorr, Phys. Rev. B **75**, 115331 (2007).

[24] J. Förstner, C. Weber, J. Danckwerts, and A. Knorr, Phys. Status Solidi B **238**, 419 (2003).

[25] M. Richter, A. Carmele, S. Butscher, N. Bücking, F. Milde, P. Kratzer, M. Scheffler, and A. Knorr, J. Appl. Phys. **105**, 122409 (2009).

[26] I. Waldmüller, J. Forstner, and A. Knorr, *Nonequilibrium Physics at Short Time Scales: Formation of Correlations* (Springer-Verlag, Berlin, 2004), pp. 251–272.

[27] F. Rossi and T. Kuhn, Rev. Mod. Phys. **74**, 895 (2002).

[28] S. Butscher, F. Milde, M. Hirtschulz, E. Malić, and A. Knorr, Appl. Phys. Lett. **91**, 203103 (2007).

[29] I. Magnúsdóttir, A. V. Uskov, S. Bischoff, B. Tromborg, and J. Mørk, J. Appl. Phys. **92**, 5982 (2002).

[30] M.-R. Dachner, J. Wolters, A. Knorr, and M. Richter, *Conference on Lasers and Electro-Optics/International Quantum Electronics Conference* (Optical Society of America, Baltimore, MD, 2009), p. JWA119.

[31] F. H. M. Faisal, *Theory of Multiphoton Processes* (Plenum, London, 1987).

[32] M. Grundmann, Physica E (Amsterdam) **5**, 167 (1999).

[33] J. Shah, *Ultrafast Spectroscopy of Semiconductors and Semiconductor Nanostructures*, Springer Series in Solid-State Sciences Vol. 115, 2nd ed. (Springer, Berlin, 1999).

[34] C. Gies, J. Wiersig, and F. Jahnke, Phys. Rev. Lett. **101**, 067401 (2008).

[35] J. P. Reithmaier, G. Sek, A. Löffler, C. Hofmann, S. Kuhn, S. Reitzenstein, L. V. Keldysh, V. D. Kulakovskii, T. L. Reinecke, and A. Forchel, Nature (London) **432**, 197 (2004).

[36] Y. Rosenwaks, M. C. Hanna, D. H. Levi, D. M. Szmyd, R. K. Ahrenkiel, and A. J. Nozik, Phys. Rev. B **48**, 14675 (1993).

[37] G. Pfanner, M. Seliger, and U. Hohenester, Phys. Rev. B **78**, 195410 (2008).